JBC Papers in Press. Published on December 27, 2018 as Manuscript RA118.006670
The latest version is at http://www.jbc.org/cgi/doi/10.1074/jbc.RA118.006670

Low metformin causes a more oxidized mitochondrial NADH/NAD redox state in hepatocytes and inhibits gluconeogenesis by a redox-independent mechanism

Ahmed Alshawi[1,2] and Loranne Agius[1*]

From the [1]Institute of Cellular Medicine, Newcastle University, Medical School, Newcastle upon Tyne NE2 4HH, UK; [2,] Kufa institute, Clinical Pathology Department, Al-Furat AL-Awsat Technical University, Iraq.

Running title: *Redox-independent inhibition of gluconeogenesis by metformin*

[*]To whom correspondence should be addressed: Loranne Agius, Institute of Cellular Medicine, Newcastle University, Medical School, Newcastle upon Tyne, NE2 4HH, UK; loranne.agius@ncl.ac.uk; Tel +441912087033

Keywords: Metformin, dimethylbiguanide, gluconeogenesis, mitochondrial glycerophosphate dehydrogenase, phosphofructokinase-1

ABSTRACT

The mechanisms by which metformin (dimethylbiguanide) inhibits hepatic gluconeogenesis at concentrations relevant for type 2 diabetes therapy remain debated. Two proposed mechanisms are: inhibition of mitochondrial Complex 1 with consequent compromised ATP and AMP homeostasis; or inhibition of mitochondrial glycerophosphate dehydrogenase (mGPDH) and thereby attenuated transfer of reducing equivalents from the cytoplasm to mitochondria resulting in a raised lactate/pyruvate ratio and redox-dependent inhibition of gluconeogenesis from reduced but not oxidised substrates. Here we show that metformin has a biphasic effect on the mitochondrial NADH/NAD redox state in mouse hepatocytes. A low cell dose of metformin (therapeutic equivalent: < 2nmol / mg) caused a more oxidized mitochondrial NADH/NAD state and an increase in lactate / pyruvate ratio, whereas a higher metformin dose (≥5nmol/mg) caused a more reduced mitochondrial NADH/NAD state similar to Complex 1 inhibition by rotenone. The low metformin dose inhibited gluconeogenesis from both oxidized (dihydroxyacetone) and reduced (xylitol) substrates by preferential partitioning of substrate towards glycolysis by a redox-independent mechanism that is best explained by allosteric regulation at phosphor-fructokinase-1 (PFK1) and/or fructose bisphosphatase-1 (FBP-1) in association with a decrease in cell glycerol 3-P, an inhibitor of PFK1 rather than by inhibition of transfer of reducing equivalents. We conclude that at a low pharmacological load, the metformin effects on the lactate / pyruvate ratio and glucose production are explained by attenuation of transmitochondrial electrogenic transport mechanisms with consequent compromised malate-aspartate shuttle and changes in allosteric effectors of PFK1 and FBP1.

Metformin (dimethylbiguanide) is the most widely prescribed drug for lowering blood glucose in type 2 diabetes (1). Its therapeutic effect is in part mediated by inhibition of hepatic glucose production (2), and is thought to involve chronic changes in gene expression (3-5) and acute inhibition of gluconeogenesis (6-8). The first mechanism that was identified for the acute suppression of gluconeogenesis was the inhibition of Complex 1 of the respiratory chain (NADH:ubiquinone oxidoreductase) with a consequent decrease in the cell ATP/ADP ratio in conjunction with a more reduced mitochondrial and cytoplasmic NADH/NAD redox state as determined from the raised ratios of 3-hydroxybutyrate / acetoacetate and lactate / pyruvate, respectively (9-13). The inhibition of gluconeogenesis was attributed to either the decrease in the cell ATP/ADP ratio (9,10,14) or to activation of AMPK resulting from the raised AMP (15). Subsequently, arguments were proposed in support of AMPK-independent mechanisms through either lowering of ATP or raised AMP (16) causing inhibition of glucagon signalling (17) or FBP1 (18) or alternatively through inhibition of mitochondrial

glycerophosphate dehydrogenase (mGPDH) (19,20). Cellular studies using high millimolar metformin concentrations and showing substantial lowering of gluconeogenesis and cell ATP are now thought to be of limited relevance because in diabetes therapy blood metformin concentrations are in the low micromolar range and substantial lowering of ATP is thought not to occur during metformin therapy (1,6).

Recently two distinct mechanisms have been proposed to explain the inhibition of gluconeogenesis by a pharmacological metformin dose of therapeutic relevance. One proposes mild elevation in AMP through compromised hepatic energy status, resulting in inhibition of glucagon signalling (17) and allosteric inhibition of FBP1 (18). The other proposes inhibition by metformin of mGPDH the key enzyme of the GP-shuttle, which is one of two shuttles that transfers reducing equivalents from the cytoplasm to the mitochondria (19,20). mGPDH is a flavin-linked mitochondrial dehydrogenase which catalyses G3P oxidation to dihydroxyacetone-P on the cytoplasmic side coupled to the reduction of FAD and transfer of electrons to the respiratory chain via ubiquinone (21). Inhibition of mGPDH by metformin is proposed to cause simultaneously a more reduced cytoplasmic NADH/NAD state evident from a higher lactate / pyruvate ratio and a more oxidised mitochondrial NADH/NAD redox state evident from a lower ratio of 3-hydroxybutyrate / acetoacetate (19,20). A key caveat to this mechanism is that it predicts inhibition of gluconeogenesis from reduced substrates (lactate and glycerol) but not from oxidised substrates (pyruvate and dihydroxyacetone) whereas the first mechanism proposing inhibition of FBP1 by AMP predicts redox-independent inhibition of gluconeogenesis from oxidised and reduced substrates. A further caveat to the second mechanism is that it predicts a more oxidized mitochondrial NADH/NAD ratio (lower 3-hydroxybutyrate / acetoacetate) as opposed to a more reduced state as occurs by inhibition of Complex 1 and as documented from hepatocyte studies with metformin (9-12). To date a more oxidised mitochondrial NADH/NAD ratio in response to metformin has only been shown in liver *in vivo* (19,20) but not in isolated hepatocytes. The aims of this study were: first, to test whether metformin has a dose-dependent effect on the mitochondrial NADH/NAD ratio in hepatocytes; second, to explore the mechanism(s) by which a low metformin dose, equivalent of the therapeutic range, affects gluconeogenesis and compare this with inhibition and/or stimulation of transfer of NADH reducing equivalents from the cytoplasm to the mitochondria by the GP-shuttle or the MA-shuttle. We report that clinically relevant doses of metformin cause a more oxidised mitochondrial NADH/NAD redox state and a more reduced cytoplasmic redox state but inhibit gluconeogenesis from oxidised substrates. This is best explained by a redox-independent mechanism involving allosteric regulation at the level of PFK1 and/or FBP1 that is in part explained by a decrease in cell glycerol 3-P an inhibitor of PFK1.

RESULTS

Biphasic effect of metformin on the mitochondrial redox state: more oxidized at low metformin

Studies *in vivo* showed that metformin causes either a more reduced (10) or a more oxidized (19,20) mitochondrial NADH/NAD redox state in liver based on the ratio of 3-hydroxybutyrate / acetoacetate which correlates with the mitochondrial NADH/NAD ratio through the hydroxybutyrate dehydrogenase equilibrium (22). Our first aim was to determine whether metformin (100-500 μM) has a dose-dependent effect on the mitochondrial NADH/NAD redox state in hepatocytes incubated with octanoate. This medium-chain fatty acid enters the mitochondria as the free acid by a mechanism independent of regulation by malonyl-CoA and thereby AMPK activity and is metabolised predominantly to acetoacetate and 3-hydroxybutyrate. We used 100 μM as the lowest metformin concentration because in hepatocytes incubated with 100 μM metformin for 2-4h metformin accumulates in the cells to 1-2 nmol / mg protein (23). This is within the range observed in mouse liver after an oral dose of 50mg metformin /kg body wt (24). At the highest concentration (500 μM) metformin accumulates to 5-10 nmol/mg (23) in rat and mouse hepatocytes. In both mouse and rat hepatocytes, high metformin (500 μM) increased the ratio of 3-hydroxybutyrate / acetoacetate as did rotenone, the Complex I inhibitor (Fig. 1A,D), and as shown previously with mM metformin in hepatocytes (9-12). However, 100 μM metformin decreased the 3-hydroxybutyrate / acetoacetate ratio (Fig.

1,A,D) indicating a more oxidised mitochondrial NADH/NAD state (22). This effect could be due to a decrease in production of NADH (if octanoate β-oxidation were inhibited) or to other mechanisms. The rate of production of acetoacetate plus 3-hydroxybutyrate was increased by 100 μM metformin in both mouse and rat hepatocytes and it was also increased by the uncoupler dinitrophenol, DNP (Fig. 1B,E), which similar to low metformin decreased the 3-hydroxybutyrate / acetoacetate ratio (Fig. 1D). This implicates a more oxidised NADH/NAD state as the primary effect of 100 μM metformin with the increase in ketone body production as secondary to the oxidized NADH/NAD ratio. When the effects of low metformin and DNP were tested in the presence of rotenone (Fig. 1G,H), only DNP lowered the 3-hydroxybutyrate / acetoacetate ratio, suggesting that the metformin effect is either upstream of the rotenone site or alternatively abolished by rotenone through other mechanisms. Although cell ATP was maintained in cells treated with metformin (Fig. 1C,F), this does not exclude small localized changes in free ATP/ADP ratio in the cytoplasm (10). We next tested for activation of AMPK by the low and high metformin concentrations from phosphorylation of the AMPK substrate, acetyl-CoA carboxylase-Ser-79 (ACC-S79) and used the small molecule AMPK activator A-769662 (10 μM) as a reference control (25) in incubations without and with octanoate in mouse hepatocytes (Fig. 1K). The high metformin concentration (500 μM) caused increased ACC phosphorylation as occurred with A-769662. Octanoate alone also increased ACC phosphorylation indicating AMPK activation. This suggests raised AMP with octanoate most likely via the acyl-CoA synthase as reported previously (26). There was lower phosphorylation of ACC by 100 μM metformin in combination with octanoate. This may be due to accelerated clearance of octanoate by 100 μM metformin.

Metformin causes greater inhibition of glucose production from dihydroxyacetone than from glycerol

Having confirmed that low metformin (100 μM) causes a more oxidised mitochondrial NADH/NAD redox state without inhibiting ketone body production we next determined the effects of 100 μM metformin on glucose production from oxidized (dihydroxyacetone, DHA) and reduced (glycerol and xylitol) substrates. Glucose production was significantly higher from DHA than from glycerol (Fig. 2). Metformin inhibited glucose production from both oxidised (DHA) and reduced (xylitol and 0.25mM glycerol) substrates and it increased the production of lactate and pyruvate with both DHA and xylitol (Fig. 2A,B). Cell ATP was unchanged by metformin with DHA but was lowered with the reduced substrates (Fig. 2C). This indicates inhibition of gluconeogenesis from both oxidised and reduced substrates by low metformin.

Low metformin but not inhibitors of the NADH shuttles favours metabolism of DHA and xylitol to glycolysis relative to glucose

To test whether inhibition of glucose production by low metformin can be explained by inhibition of NADH shuttles we compared 100 μM metformin with aminooxyacetate (AOA), an inhibitor of the malate-aspartate shuttle (MA-shuttle) (27), or GPi (STK017597, GPI), a recently identified inhibitor (28) of the GP-shuttle, on metabolism of DHA (Fig. 3A-F) or xylitol (Fig. 3G-L) in either the absence (open bars) or presence (shaded bars) of octanoate as a source of mitochondrial NADH. Metformin inhibited glucose production and increased lactate plus pyruvate production without affecting total metabolism to glucose plus pyruvate and lactate from DHA (Fig. 3A-C) or xylitol (Fig.3 G-I). Accordingly, metformin decreased the fractional partitioning of DHA and xylitol to glucose relative to glycolysis (Fig 3D, Fig 3J). Octanoate (shaded bars) had opposite effects from metformin and increased partitioning of DHA and xylitol to glucose relative to glycolysis with no significant effect on total metabolism (Fig. 3A-D; 3G-J). Both the lactate/pyruvate ratio and cell G3P were higher with the reduced substrate xylitol (Fig. 3KL) than with DHA (Fig. 3EF), as expected (29), and octanoate increased the lactate/pyruvate ratio with DHA (Fig. 3E) but not with xylitol (Fig. 3K). Metformin increased the lactate/pyruvate ratio with both DHA and xylitol but decreased G3P (Fig. 3EK; Fig. 3FL). The MA-shuttle inhibitor, AOA caused a large increase in the lactate/pyruvate ratio, as expected (27), but the GPi had a smaller effect than AOA. Unlike metformin, AOA increased G3P (Fig. 3FL) and did not decrease partitioning of DHA to glucose.

AOA decreased total metabolism of the reduced substrate xylitol to glucose, pyruvate and lactate (Fig. 3I). Cumulatively, these results support the following conclusions. First, that low metformin inhibited glucose production from both oxidized (DHA) and reduced (xylitol) substrates by increasing partitioning to glycolysis, with a concomitant increase in lactate / pyruvate ratio and a decrease in cell G3P. Second, that AOA which caused a more reduced cytoplasmic redox state (lactate / pyruvate ratio) than metformin did not mimic the metformin inhibition of gluconeogenesis from DHA but it decreased total xylitol metabolism and increased cell G3P. Third, that the inhibitor of mGPDH (GPi 20μM) was less effective than the MA-shuttle inhibitor (AOA) in raising the lactate / pyruvate ratio and did not raise cell G3P, the substrate of mGPDH. Fourth, that octanoate which promotes an increase in lactate/pyruvate ratio with DHA but not with xylitol had opposite effects from metformin on the directionality of flux between glycolysis and gluconeogenesis with both DHA and xylitol as substrates.

GPi (STK017597) but not metformin inhibits endogenous mGPDH activity in hepatocytes

The greater effect of the MA-shuttle inhibitor (AOA) compared with the mGPDH inhibitor (GPi, STK017597) on the lactate/pyruvate ratio could be due to either a greater contribution of the MA-shuttle compared with the GP-shuttle to transfer of reducing equivalents from the cytoplasm to mitochondria, or to poor efficacy or cellular uptake of GPi by hepatocytes. We next tested the effects of the GPi and metformin on mGPDH activity in permeabilised hepatocytes using the electron acceptor dichlorophenol indophenol (31) and confirmed inhibition of mGPDH activity by 10-80 μM GPi (Fig. 4A) as reported previously (28), but not with metformin at 0.1 to 5 mM (Fig. 4B). Although STK017597 is a potent mGPDH inhibitor in permeabilised hepatocytes, it may be ineffective in the intact hepatocytes because of slow transport or low functional GP-shuttle activity. In additional experiments with 80 μM GPi in hepatocytes that were either untreated or treated with an adenoviral vector to overexpress mGPDH (Fig.5) there was an increase in G3P with 80 μM GPi in the untreated hepatocytes consistent with endogenous functional mGPDH activity (Fig. 5A). However partitioning of DHA to glucose was not inhibited by 80 μM GP (Fig. 5B-E).

Overexpression of mGPDH lowers cell G3P and promotes a more reduced mitochondrial NADH/NAD ratio and increased glycolysis

To further test the role of the GP-shuttle in glycolysis and gluconeogenesis we used adenoviral vectors for overexpression of mGPDH or shRNA knock-down in mouse hepatocytes and confirmed an increase or decrease, respectively in *Gpd2* mRNA after 24h (Fig. 4C). We also confirmed overexpression of mGPDH protein by immunoblotting and the activity assay with 2 adenoviral titres (Fig. 4D,E) but there was little suppression of mGPDH activity by sh-RNA knock-down, presumably because of the long half-life of mGPDH protein (21). We therefore used two levels of mGPDH overexpression (as in Fig. 4D,E) for metabolic studies (Fig. 6-8). With 25mM glucose and octanoate as substrates mGPDH overexpression was associated with lower levels of cell G3P (Fig. 6A) and with a more reduced mitochondrial NADH/NAD redox state (Fig. 6B), but decreased production of ketone bodies (Fig. 6C) and thereby β-oxidation of octanoate. The production of lactate and pyruvate was slightly raised (Fig. 6D) with negligible change in the lactate / pyruvate ratio (Fig. 6E). The more reduced mitochondrial NADH/NAD redox state in conjunction with lower cell G3P confirms that overexpressed mGPDH is appropriately targeted to the mitochondrial membrane and is functional such that G3P oxidation is associated with transfer of reducing equivalents to mitochondria and presumably reversed electron transport resulting in both a raised NADH/NAD and suppression of β-oxidation. Inhibition of the MA-shuttle with AOA, unlike overexpression of mGPDH, had negligible effect on the mitochondrial redox state but it counteracted and reversed the effect of low metformin on the mitochondrial redox state (Fig. 1-I,J).

Overexpression of mGPDH promotes DHA metabolism to glycolysis rather than glucose and does not increase xylitol metabolism

A role for mGPDH in the control of gluconeogenesis has previously been inferred from lower blood glucose in some mouse models of *Gpd2* deficiency (19,20,32-34) and

from association studies in hepatocytes from rodents with altered thyroid hormone signalling and raised mGPDH activity (35). In the latter study (35) mGPDH was one of a number of genes showing altered expression with thyroid status. To test the specific role of mGPDH in control of gluconeogenesis, we determined the effects of mGPDH overexpression on rates of glucose production from oxidised and reduced substrates. With DHA as substrate (Fig. 7A-F), overexpression of mGPDH was associated with lower cell G3P, and increased production of pyruvate plus lactate but not glucose or total DHA metabolism and accordingly with decreased partitioning of DHA to glucose (Fig. 7A-E). This was associated with a raised lactate / pyruvate ratio (Fig. 7F). Likewise with DHA plus octanoate in incubations without or with AOA, to inhibit the MA-shuttle (Fig. 7G-L), there was also lowering of G3P and increased production of pyruvate plus lactate and decreased partitioning of DHA to glucose with mGPDH overexpression. With xylitol as substrate and without or with AOA to inhibit the MA-shuttle (Fig. 8A-C), both cell G3P and the lactate to pyruvate ratio were markedly elevated by MA-shuttle inhibitor and total xylitol metabolism was inhibited indicating an essential role for the MA-shuttle in regenerating NAD consumed by xylitol oxidation to xylulose. Overexpression of mGPDH markedly lowered cell G3P but did not reverse the AOA effect on total xylitol metabolism and had negligible effect on the lactate /pyruvate ratio (Fig. 8A-C).

Overexpression of mGPDH increases total metabolism of glycerol

We next determined the effects of mGPDH overexpression on glycerol metabolism (Fig. 8D-I). Cell G3P was markedly lowered and total glycerol metabolism to glucose, pyruvate and lactate was increased mainly as a result of an increase in pyruvate and lactate production (Fig. 8D-G). Increased mGPDH activity favoured increased glycerol metabolism by preferential partitioning to glycolysis relative to glucose (Fig. 8H). Cumulatively, overexpression of mGPDH caused: a marked decrease in cell G3P with all substrates tested (glucose, DHA, xylitol, glycerol), (Figs 6-8), and a more reduced mitochondrial NADH/NAD state (Fig. 6). With DHA as substrate the effects of mGPDH overexpression (Fig. 7) mimicked the effect of metformin (Fig. 3) in favouring partitioning to glycolysis relative to glucose.

Metformin inhibition of gluconeogenesis from DHA is abolished by allosteric targeting at PFK1 and FBP1

The above studies suggest that the metformin inhibition of glucose production from DHA and xylitol (Fig 3), which occurs in conjunction with lowering of cell G3P is not mimicked by inhibition of either the MA-shuttle (Fig. 3) or the GP-shuttle (Fig. 5). We next considered allosteric regulation at PFK1 and/or FBP1 as a candidate mechanism for the effect of low metformin on glycolysis and gluconeogenesis because previous work showed that the inhibition of glycolysis by octanoate is in part explained by raised citrate, a potent inhibitor of PFK1 (36,37). To test for regulation at PFK1 or FBP1 we expressed a kinase-deficient variant (PFK-KD) of the bifunctional enzyme PFK2/FBP2, which depletes cell fructose 2,6-P_2 (38), a potent activator of PFK1 and inhibitor of FBP1 (39) and we compared metformin (100 μM) with the activator of AMPK (A-769662, 10 μM) in cells that were either untreated or depleted of fructose 2,6-P_2 (Fig. 9, open vs shaded bars). Depletion of fructose 2,6-P_2 (with Adv-PFK-KD) increased glucose production and decreased glycolysis consistent with decreased PFK1 and increased FBP1 activity (39). In untreated cells metformin (100μM) and A-769662 had opposite effects (inhibition and stimulation, respectively) on relative partitioning of DHA to glucose (Fig 9 A-D). These effects of metformin and A-769662 were attenuated by fructose 2,6-P_2 depletion (Fig 9, shaded bars). Cumulatively, this shows that the metformin effect is not mimicked by activation of AMPK and is attenuated by depletion of fructose 2,6-P_2 an allosteric regulator of both PFK1 and FBP1. We next used an inhibitor of FBP1 that binds to the AMP-site (40) and a citrate analogue inhibitor of PFK1 (ATA, aurintricarboxylic acid) which antagonizes activation of PFK1 by AMP and fructose 2,6-P_2 (41), to selectively target FBP1 or PFK1 (Fig. 10). For these studies we used the chlorogenic acid derivative, S4048 (200nM) which is a selective inhibitor of the G6P transporter Slc37a4 (42), to raise cell G6P which is otherwise below detection limits in hepatocytes incubated in glucose-free medium. The FBP1 inhibitor, lowered glucose production from DHA and cell G6P whereas the PFK1 inhibitor raised glucose production and G6P (Fig. 10A,B). The PFK1 inhibitor caused partitioning

of substrate towards glucose despite attenuation of total DHA metabolism (Fig. 10C-E). The inhibition of gluconeogenesis and the lowering of cell G6P by metformin were abolished by the PFK1 and FBP1 inhibitors (Fig. 10A,B). Cumulatively, this points to a significant contribution of allosteric control of PFK1 and FBP1 in the partitioning of DHA metabolism between glycolysis and gluconeogenesis and in the metformin inhibition of glucose production.

DISCUSSION

Although metformin has been used for Type 2 diabetes therapy for several decades (1,2), the mechanisms by which it inhibits hepatic gluconeogenesis remain debated (4-20). Two contentious issues are: what metformin exposure in cellular models is the equivalent of therapeutic exposure in human diabetes (1,5,18) and whether the acute inhibition of gluconeogenesis is explained by compromised energy status via inhibition of Complex 1 (9-18) or by a redox-dependent mechanism through inhibition of mGPDH and thereby the GP-shuttle (19,20).

The MA-shuttle and the GP-shuttle together with production of lactate by lactate dehydrogenase are the three major mechanisms in liver that lead to the regeneration of NAD that is consumed in glycolysis (Fig. 11). Flux through the GP-shuttle is determined by the activity of mGPDH, which is expressed at relatively low levels in liver compared with brain, muscle and thermogenic brown adipose tissue (21). Nonetheless it is adaptively regulated in liver by thyroid and steroid hormone status and it is also allosterically regulated by Ca^{2+} (21). Altered activity of mGPDH could therefore result in variable contribution of this shuttle to the cytoplasmic and mitochondrial redox state. Mice with selective disruption of either the GP-shuttle by knock-down of mGPDH or the MA-shuttle by knock-down of citrin, the electrogenic aspartate transporter, have a modest phenotype with respect to fasting blood glucose (32-34), though with a greater role of the MA-shuttle compared with GP-shuttle in lowering blood glucose (34). However combined knock-down of both mGPDH and citrin resulted in significant disruption of blood glucose and glycerol levels, indicating that both shuttles can mutually compensate when either shuttle is genetically deleted (34). In the present study we used inhibitors of the MA-shuttle and GP-shuttle and we overexpressed mGPDH to explore the role of these shuttles in the maintenance of cytoplasmic and mitochondrial NADH/NAD redox state and metabolism of oxidized and reduced substrates. We show that inhibition of the MA-shuttle causes a more reduced cytoplasmic redox state but with negligible effect on the mitochondrial redox state whereas overexpression of mGPDH causes a more reduced mitochondrial redox state, but with variable effects on the lactate / pyruvate ratio depending on the substrate conditions. We used a metformin concentration and exposure time in hepatocytes, that results in cellular metformin levels (1-2 nmol/mg) (23) that are attained in mouse liver after an oral metformin dose equivalent to the therapeutic dose (50mg/kg or 3g per 60kg) (24). Two key findings from the present study are, first that low metformin promotes a decrease in 3-hydroxybutyrate/ acetoacetate ratio (more oxidized mitochondrial NADH/NAD) but an increase in lactate/ pyruvate ratio (more reduced cytoplasmic NADH/NAD) as with a low dose of metformin *in vivo* in liver (19,20) and kidney (43,44); second, that low metformin inhibits gluconeogenesis from oxidized and reduced substrates by preferential partitioning to glycolysis and with concomitant lowering of cell G3P. This inhibition of gluconeogenesis cannot be explained by inhibition of either the MA-shuttle or the GP-shuttle and is best explained by allosteric regulation at the level of PFK1 and FBP1. These two effects of metformin are discussed separately.

The increase in lactate/pyruvate ratio is probably the most widely documented effect of metformin *in vivo* (19,20,43) and *in vitro* (9-12,14). Although an increase in lactate/ pyruvate ratio by a high metformin dose is frequently attributed to inhibition of Complex I and thereby the respiratory chain, the increase by low metformin in conjunction with a more oxidized mitochondrial NADH/NAD state requires other explanations. One possible explanation for this is inhibition of mGPDH (19,20). However, in this study cell G3P, the substrate of mGPDH was lowered by metformin and by mGPDH overexpression and was increased with the mGPDH inhibitor. This does not support a role for inhibition of GP-shuttle activity by metformin and accordingly other explanations need to be considered for the increase in lactate/pyruvate ratio by low

metformin. Flux through the MA-shuttle involves an electrogenic transporter for aspartate and is highly dependent on mitochondrial membrane potential (45-48). The most plausible explanation for the increase in lactate / pyruvate ratio by low metformin is that it results from accumulation of metformin in mitochondria with consequent mitochondrial depolarisation (9,49) and inhibition of the MA-shuttle (45-48) through attenuation of electrogenic transport (Fig. 11). The biphasic effect of metformin on the ratio of 3-hydroxybutyrate / acetoacetate in hepatocytes suggests that metformin inhibits Complex I at the higher concentration which corresponds to a cell load ≥ 5 nmol metformin / mg cell protein but not at 100 μM which corresponds to ≤2nmol metformin / mg protein. A key question is what is the mechanism for the oxidized mitochondrial NADH/NAD state by low metformin? Detailed studies by Bridges and colleagues (13) on the effects of metformin on the sequential reactions of complex 1 (NADH oxidation, electron transfer and ubiquinone reduction) showed that metformin interacts with at least two sites, the flavin site and the ubiquinone site. Metformin activates the first reaction, NADH oxidation when this is coupled to the artificial electron acceptor FeCN but it inhibits reversibly at the ubiquinone site by a distinct mechanism from canonical Complex I inhibitors (e.g. rotenone) which bind irreversibly. Whether low metformin concentrations (below the threshold for inhibition of the ubiquinone site) could lower the NADH/NAD ratio through metformin's effect at the flavin site is speculative because the rate constant for NADH oxidation is far higher than for ubiquinone reduction (50). A simpler explanation is that depolarisation of the mitochondria by metformin accumulation in mitochondria accounts for the lower NADH/NAD ratio by increased flux through Complex I as occurs during depolarisation with the uncoupler dinitrophenol because flux through Complex 1 is impeded by the proton motive force. Accordingly mitochondrial depolarisation by metformin accumulation could in principle account for both the oxidized mitochondrial redox state and the reduced cytoplasmic redox state.

We show in this study that the inhibition of gluconeogenesis by the low dose of metformin cannot be explained by either inhibition of Complex 1, (because of the more oxidized mitochondrial redox state) or activation of AMPK, (because AMPK activation has the converse effect on DHA metabolism from metformin) or by inhibition of transfer of reducing equivalents from the cytoplasm to the mitochondria because inhibition of these shuttles does not mimic metformin on DHA metabolism. Based on the large effects of the inhibitors of PFK1 and FBP1 or by depletion of fructose 2,6-P_2 , the allosteric regulator of both PFK1 and FBP1 that acts synergistically with other effectors (39), on the directionality of flux between glycolysis versus gluconeogenesis and also the attenuation of the metformin effect by these inhibitors, we propose that allosteric regulation at the level of PFK1 and FBP1 is the most plausible explanation for the metformin effect on gluconeogenesis and glycolysis. FBP1 is regulated synergistically by AMP and fructose 2,6-P_2 and PFK1 is regulated by multiple positive effectors (e.g. AMP, fructose 2,6-P_2, fructose 1,6-P_2, glucose 1,6-P_2 and Pi) and negative effectors (ATP, citrate, G3P) (39). If the increase in the lactate/pyruvate ratio by low metformin is consequent to mitochondrial depolarisation and inhibition of the electrogenic transporter of the MA-shuttle (45-48), then other electrogenic transport mechanisms would likewise be expected to be attenuated. One such mechanism is the adenine nucleotide transporter (ANT) which exchanges ADP^{3-} on the cytoplasmic side for ATP^{4-} on the mitochondrial side (51,52). An increase in the cytoplasmic ADP/ATP ratio would be expected to result from mitochondrial depolarisation. Other allosteric effectors of PFK1 which may contribute to stimulation of glycolysis include citrate which is a potent PFK1 inhibitor and has been shown to be lowered by metformin treatment in some models of diabetes (53) and G3P which is a potent inhibitor of PFK1 (54). In this study cell G3P was decreased by low metformin in conditions of raised glycolysis and decreased gluconeogenesis and likewise G3P was decreased in cells overexpressing mGPDH which showed similar partitioning of DHA towards glycolysis as with metformin. The lowering of cell G3P by metformin in conditions of raised lactate / pyruvate ratio may result from increased flux through the GP-shuttle in conditions of impaired MA-shuttle flux because of mitochondrial depolarisation. The more reduced mitochondrial redox state by metformin in the presence of the MA-shuttle inhibitor supports this explanation. Cumulatively, this

supports the conclusion that low metformin concentrations which do not inhibit Complex I, can inhibit gluconeogenesis by a redox independent mechanism through allosteric regulation of PFK1 and FBP1 in conjunction with lowering of cell G3P and an increase in lactate /pyruvate ratio. The latter effects may be due to altered flux through the MA-shuttle and GP-shuttle (inhibition and stimulation, respectively).

Experimental procedures

Reagents: STK017597 (GPI), an inhibitor of mGPDH (28) was from Vitas-M Laboratory; A-769662 was from Tocris Biosciences; the FBP1 inhibitor, (5-chloro-2-[N-(2,5dichlorobenzene sulfonamide)]-benzoxazole (40) was from Calbiochem/Santa cruz. S4048, the chlorogenic acid derivative (1-[2-(4-chloro-phenyl)-cyclopropylmethoxy]-3, 4-dihydroxy-5-(3-imidazo[4,5-b]pyridin-1-yl-3-phenyl-acryloyloxy)-cyclohexanecarboxylic acid) (42) was a kind gift from Sanofi-Aventis. All other reagents were from Sigma.

Adenoviral vectors: for overexpression of mouse mGPDH (Ad-m-Gpd2, ADV-279685; RefSeq BC021359) and for sh-RNA knock-down (ADV-m-Gpd2-shRNA, shADV-279685; RefSeq NM-010274) were generated by Vector Biolabs, Malvern, PA 19355. The adenoviral vector for expression of a kinase-deficient variant of PFKFB1 (S32D, T55V) denoted by PFK-KD for a bisphosphatase-active kinase-deficient variant of 6-phosphofructo-2-kinase–fructose-2,6-bisphosphatase was described in (38).

Hepatocyte isolation and culture: Hepatocytes were isolated by collagenase perfusion of the liver either from adult male Wistar rats (200-280 g body wt) or from adult male C57BL/6JOlaHsd mice (20-30 g body wt) obtained from Harlan/Envigo (Bicester UK). Unless otherwise indicated mouse hepatocytes were used. Rat and mice were housed in environmental conditions as outlined in the Home Office Code or Practice. Procedures conformed to Home Office Regulations and were approved by the Newcastle University Ethics Committee. Rat hepatocytes were isolated at previously described (38). For mouse hepatocyte isolation, euthanasia was by isoflurane overdose followed by heparin injection and laparotomy. The liver was perfused at 5 ml/min for 5 min with Ca-free Hanks buffer followed by 20 min with Hanks buffer containing 0.1mg/ml collagenase (Sigma C5138). After sedimentation at 50g the hepatocytes were suspended in Minimum Essential Medium (MEM, Life Technologies 21430) supplemented with 5% (v/v) newborn calf serum and 10nM dexamethasone and 10nM insulin and seeded on gelatin-coated (0.1% wt/vol) multi-well plates. After cell attachment the medium was replaced by serum-free MEM containing 5mM glucose, 10nM dexamethasone, 1nM insulin and the hepatocytes were cultured overnight (~16-20 h).

Treatment with adenoviral vectors: For protein overexpression 2h after cell attachment the serum-containing medium was replaced by serum-free MEM containing Ad-m-Gpd2 (ADV-279685; Ref Seq BC021359, Vector Biolabs Malvern, PA) at titres of 1.6 and 4.8 x 10^7 PFU/ml for overexpression of mouse mGPDH or with PFK-KD for expression of a kinase-deficient variant of PFK2/FBP2 (Pfkfb1: S32D, T55V) for depletion of fructose 2,6-P_2 (38). After 4h the medium was replaced by serum-free MEM containing 10nM dexamethasone and 1nM insulin and the hepatocytes were cultured for 18-20h.

Hepatocyte incubations with metformin: All experiments with metformin were performed after 16-20h culture with the exception of Fig 1G to 1J, which was started 3h after cell plating. The hepatocyte monolayers were pre-incubated with metformin for 2h with either MEM containing 5 mM glucose or glucose-free DMEM (Life technologies, A14430). After 2h the medium was replaced by fresh MEM or glucose-free DMEM medium with the same metformin concentrations and other substrates (e.g. octanoate and gluconeogenic precursors) as indicated for either 1h (acetoacetate + 3-hydroxybutyrate) or 2h (glucose production studies). On termination of the incubations the medium was collected for determination of acetoacetate, 3-hydroxybutyrate, lactate, pyruvate and glucose and the hepatocyte monolayers were snap-frozen in liquid nitrogen and stored at -80°C until analysis.

Metabolite assays: For determination of ketone bodies and pyruvate the medium was acidified with 0.2 volume of 0.6M $HClO_4$. Acetoacetate and 3-hydroxybutyrate were assayed using 3-hydroxybutyrate dehydrogenase and pyruvate and lactate using lactate dehydrogenase from the change in NADH fluorescence (Ex 340, Em 460) as in (55). Ketone body production is expressed as nmol / h per mg protein (mouse hepatocytes) or as % control (rat hepatocytes Fig. 1D-F). Glucose was determined by the hexokinase, glucose 6-phosphate dehydrogenase coupled assay (56). Production of pyruvate plus lactate or glucose are expressed as nmol / 2h per mg protein and glucose production is also expressed as % of total production of pyruvate + lactate + glucose (expressed as C3 units). For determination of cell ATP, G3P and G6P the hepatocyte monolayers were extracted 2.5% (wt/vol) 5-sulfosalicylic acid and deproteinized by sedimentation at 10,000g, 10min. The supernatant was neutralised with 1M-KOH, 0.66M-K_2HPO_4 and cell ATP was determined by a luciferase coupled luminometric method (Sigma FLAA), G6P and G3P were assayed using glucose 6-phosphate dehydrogenase and glycerol 3-phosphate dehydrogenase, respectively by coupling to resazurin conversion to resorufin with diaphorase (Ex 530, Em 590) (57). Standards for the assays were prepared fresh in culture medium or 2.5% 5-sulfosalicylic acid and concentrations were determined from standard curves and expressed as nmol / mg protein determined by the Lowry assay.

Activity of mGPDH was determined on hepatocyte monolayers that were snap-frozen in liquid nitrogen and stored at -80^{o}C until analysis. The assay medium containing 200mM sucrose, 50mM KPi pH 7.6, 200 µM DCIP and 25mM DL-G3P and activity was determined from the decrease in absorbance at 600 nm using the extinction in (31).

Western blotting: Immunoactivity to mouse mGPDH (Proteintech, #17219-1Ap); GAPDH (Hytest ABIN153387); and ACC-ser-79(P) (Cell Signalling #11818) were determined by SDS-PAGE using 8% (ACC) or 12% (Gpd2) SDS and immunoblotting. They were quantified by densitometry.

RNA analysis: RNA was extracted with Trizol and cDNA synthesized by MMLV. The primers used for real-time RT-PCR were: Gpd2, Forward, ACTACCTGAGTTCTGACGTTG AAG; reverse, TAACAAGGGGACGGATAC CA; Gapdh, forward, GAC AAT GAA TAC GGCTACAGCA; reverse GGC CTC TCT TGCTCAGTGTC.

Statistical analysis. Results for all data sets other than Figure 2 are expressed as means ± SD for the number of hepatocyte preparations indicated and statistical analysis was either by the Student's paired t-test or by one-way ANOVA. For Figure 2 the data represents replicate incubations in a single hepatocyte preparation.

Acknowledgements: We are very grateful to Dr. Judy Hirst for her advice on the manuscript.

Conflict of interest: The authors declare that they have no conflicts of interest with the contents of this article.

Author contributions: AA and LA designed the experiments. AA performed the experiments and the analysis. LA with AA wrote the paper.

References

1. Bailey CJ. (2017) Metformin: historical overview. *Diabetologia.* **60,** 1566-1576
2. Natali A, Ferrannini E. (2006) Effects of metformin and thiazolidinediones on suppression of hepatic glucose production and stimulation of glucose uptake in type 2 diabetes: a systematic review. *Diabetologia*. **49**, 434-41
3. Heishi M, Ichihara J, Teramoto R, Itakura Y, Hayashi K, Ishikawa H, Gomi H, Sakai J, Kanaoka M, Taiji M, Kimura T. (2006) Global gene expression analysis in liver of obese diabetic db/db mice treated with metformin. *Diabetologia*. **49,** 1647-55
4. Cao J, Meng S, Chang E, Beckwith-Fickas K, Xiong L, Cole RN, Radovick S, Wondisford FE, He L. (2014) Low concentrations of metformin suppress glucose production in hepatocytes through AMP-activated protein kinase (AMPK). *J Biol Chem.* **289,** 20435-46
5. He L, Wondisford FE. (2015) Metformin action: concentrations matter. Cell Metab. **21,** 159-162
6. Foretz M, Guigas B, Bertrand L, Pollak M, Viollet B. Metformin: from mechanisms of action to therapies. *Cell Metab.* 2014;20:953-66
7. Baur JA, Birnbaum MJ. (2014) Control of gluconeogenesis by metformin: does redox trump energy charge? *Cell Metab.* **20,** 197-9
8. Rena G, Hardie DG, Pearson ER. (2017) The mechanisms of action of metformin. *Diabetologia.* **60**, 1577-1585
9. El-Mir MY, Nogueira V, Fontaine E, Avéret N, Rigoulet M, Leverve X. (2000) Dimethylbiguanide inhibits cell respiration via an indirect effect targeted on the respiratory chain complex I. *J Biol Chem.* **275,** 223-8
10. Owen MR, Doran E, Halestrap AP. (2000) Evidence that metformin exerts its anti-diabetic effects through inhibition of complex 1 of the mitochondrial respiratory chain. *Biochem J.* **348,** 607-14
11. Fulgencio JP, Kohl C, Girard J, Pégorier JP. (2001) Effect of metformin on fatty acid and glucose metabolism in freshly isolated hepatocytes and on specific gene expression in cultured hepatocytes. *Biochem Pharmacol.* **62,** 439-46
12. Gouaref I, Detaille D, Wiernsperger N, Khan NA, Leverve X, Koceir EA. (2017) The desert gerbil Psammomys obesus as a model for metformin-sensitive nutritional type 2 diabetes to protect hepatocellular metabolic damage: Impact of mitochondrial redox state. *PLoS One.* **12:** e0172053
13. Bridges HR, Jones AJ, Pollak MN, Hirst J. (2014) Effects of metformin and other biguanides on oxidative phosphorylation in mitochondria. *Biochem J.* **462,** 475-87
14. Argaud D, Roth H, Wiernsperger N, Leverve XM. (1993) Metformin decreases gluconeogenesis by enhancing the pyruvate kinase flux in isolated rat hepatocytes. *Eur J Biochem.* **213,** 1341-8
15. Zhou G, Myers R, Li Y, Chen Y, Shen X, Fenyk-Melody J, Wu M, Ventre J, Doebber T, Fujii N, Musi N, Hirshman MF, Goodyear LJ, Moller DE. (2001) Role of AMP-activated protein kinase in mechanism of metformin action. *J Clin Invest.* **108,** 1167-74
16. Foretz M, Hébrard S, Leclerc J, Zarrinpashneh E, Soty M, Mithieux G, Sakamoto K, Andreelli F, Viollet B. (2010) Metformin inhibits hepatic gluconeogenesis in mice independently of the LKB1/AMPK pathway via a decrease in hepatic energy state. *J Clin Invest.* **120,** 2355-69
17. Miller RA, Chu Q, Xie J, Foretz M, Viollet B, Birnbaum MJ. (2013) Biguanides suppress hepatic glucagon signalling by decreasing production of cyclic AMP. *Nature.* **494,** 256-60
18. Hunter RW, Hughey CC, Lantier L, Sundelin EI, Peggie M, Zeqiraj E, Sicheri F, Jessen N, Wasserman DH, Sakamoto K. (2018) Metformin reduces liver glucose production by inhibition of fructose-1-6-bisphosphatase. *Nat Med*. **24,** 1395-1406
19. Madiraju AK, Erion DM, Rahimi Y, Zhang XM, Braddock DT, Albright RA, Prigaro BJ, Wood JL, Bhanot S, MacDonald MJ, Jurczak MJ, Camporez JP, Lee HY, Cline GW, Samuel VT, Kibbey RG, Shulman GI. (2014) Metformin suppresses gluconeogenesis by inhibiting mitochondrial glycerophosphate dehydrogenase. *Nature*. **510,** 542-6
20. Madiraju AK, Qiu Y, Perry RJ, Rahimi Y, Zhang XM, Zhang D, Camporez JG, Cline GW, Butrico GM, Kemp BE, Casals G, Steinberg GR, Vatner DF, Petersen KF, Shulman GI. (2018) Metformin inhibits gluconeogenesis via a redox-dependent mechanism in vivo. *Nat Med.* **24,** 1384-1394
21. Mráček T, Drahota Z, Houštěk J. (2013) The function and the role of the mitochondrial glycerol-3-phosphate dehydrogenase in mammalian tissues. *Biochim Biophys Acta.* **1827,** 401-10

22. Williamson DH, Lund P, Krebs HA. (1967) The redox state of free nicotinamide-adenine dinucleotide in the cytoplasm and mitochondria of rat liver. *Biochem J.* **103,** 514-27
23. Al-Oanzi ZH, Fountana S, Moonira T, Tudhope SJ, Petrie JL, Alshawi A, Patman G, Arden C, Reeves HL, Agius L. (2017) Opposite effects of a glucokinase activator and metformin on glucose-regulated gene expression in hepatocytes. Diabetes Obes Metab. **19,** 1078-1087
24. Wilcock C, Bailey CJ. (1994) Accumulation of metformin by tissues of the normal and diabetic mouse. *Xenobiotica.* **24,** 49-57
25. Cool B, Zinker B, Chiou W, Kifle L, Cao N, Perham M, Dickinson R, Adler A, Gagne G, Iyengar R, Zhao G, Marsh K, Kym P, Jung P, Camp HS, Frevert E. (2006) Identification and characterization of a small molecule AMPK activator that treats key components of type 2 diabetes and the metabolic syndrome. Cell Metab. 3, 403-16
26. Kawaguchi T, Osatomi K, Yamashita H, Kabashima T, Uyeda K. (2002) Mechanism for fatty acid "sparing" effect on glucose-induced transcription: regulation of carbohydrate-responsive element-binding protein by AMP-activated protein kinase. J Biol Chem. 277, 3829-35
27. Berry MN, Gregory RB, Grivell AR, Phillips JW, Schön A. (1994) capacity of reducing-equivalent shuttles limits glycolysis during ethanol oxidation. Eur J Biochem. **225,** 557-64
28. Orr AL, Ashok D, Sarantos MR, Ng R, Shi T, Gerencser AA, Hughes RE, Brand MD. (2014) Novel inhibitors of mitochondrial sn-glycerol 3-phosphate dehydrogenase. *PLoS One*. **9:** e89938
29. Vincent MF, Van den Berghe G, Hers HG. (1989) D-xylulose-induced depletion of ATP and Pi in isolated rat hepatocytes. *FASEB J.* **3,** 1855-61
30. Berry MN, Gregory RB, Grivell AR, Phillips JW, Schön A. (1994) The capacity of reducing-equivalent shuttles limits glycolysis during ethanol oxidation. *Eur J Biochem.* **225**, 557-64
31. Dawson AP, Thorne CJ. (1969) Preparation and some properties of L-3-glycerophosphate dehydrogenase from pig brain mitochondria. *Biochem J.* **111,** 27-34
32. Brown LJ, Koza RA, Everett C, Reitman ML, Marshall L, Fahien LA, Kozak LP, MacDonald MJ. (2002) Normal thyroid thermogenesis but reduced viability and adiposity in mice lacking the mitochondrial glycerol phosphate dehydrogenase. *J Biol Chem.* **277,** 32892-8
33. Barberà A, Gudayol M, Eto K, Corominola H, Maechler P, Miró O, Cardellach F, Gomis R. (2003) A high carbohydrate diet does not induce hyperglycaemia in a mitochondrial glycerol-3-phosphate dehydrogenase-deficient mouse. *Diabetologia.* **46,** 1394-401
34. Saheki T, Iijima M, Li MX, Kobayashi K, Horiuchi M, Ushikai M, Okumura F, Meng XJ, Inoue I, Tajima A, Moriyama M, Eto K, Kadowaki T, Sinasac DS, Tsui LC, Tsuji M, Okano A, Kobayashi T. (2007) Citrin/mitochondrial glycerol-3-phosphate dehydrogenase double knock-out mice recapitulate features of human citrin deficiency. *J Biol Chem.* **282,** 25041-52
35. Taleux N, Guigas B, Dubouchaud H, Moreno M, Weitzel JM, Goglia F, Favier R, Leverve XM. (2009) High expression of thyroid hormone receptors and mitochondrial glycerol-3-phosphate dehydrogenase in the liver is linked to enhanced fatty acid oxidation in Lou/C, a rat strain resistant to obesity. *J Biol Chem.* **284,** 4308-16
36. Nomura T, Iguchi A, Sakamoto N, Harris RA. (1983) Effects of octanoate and acetate upon hepatic glycolysis and lipogenesis. *Biochim Biophys Acta.* **754,** 315-20
37. Williamson JR, Browning ET, Scholz R. (1969) Control mechanisms of gluconeogenesis and ketogenesis. I. Effects of oleate on gluconeogenesis in perfused rat liver. *J Biol Chem.* **244,** 4607-16
38. Arden C, Tudhope SJ, Petrie JL, Al-Oanzi ZH, Cullen KS, Lange AJ, Towle HC, Agius L. (2012) Fructose 2,6-bisphosphate is essential for glucose-regulated gene transcription of glucose-6-phosphatase and other ChREBP target genes in hepatocytes. *Biochem J.* **443,** 111-23
39. Hers HG, Hue L. (1983) Gluconeogenesis and related aspects of glycolysis. *Annu Rev Biochem.* **52,** 617-53
40. Dang Q, Brown BS, Liu Y, Rydzewski RM, Robinson ED, van Poelje PD, Reddy MR, Erion MD. (2009) Fructose-1,6-bisphosphatase inhibitors. 1. Purine phosphonic acids as novel AMP mimics. *J Med Chem.* **52,** 2880-98
41. McCune SA, Foe LG, Kemp RG, Jurin RR. (1989) Aurintricarboxylic acid is a potent inhibitor of phosphofructokinase. *Biochem J.* **259,** 925-7
42. Härndahl L, Schmoll D, Herling AW, Agius L. (2006) The role of glucose 6-phosphate in mediating the effects of glucokinase overexpression on hepatic glucose metabolism. *FEBS J.* **273,** 336-46
43. Qi H, Nielsen PM, Schroeder M, Bertelsen LB, Palm F, Laustsen C. (2018) Acute renal metabolic effect of metformin assessed with hyperpolarised MRI in rats. *Diabetologia.* **61**, 445-454

44. von Morze C, Ohliger MA, Marco-Rius I, Wilson DM, Flavell RR, Pearce D, Vigneron DB, Kurhanewicz J, Wang ZJ. (2108) Direct assessment of renal mitochondrial redox state using hyperpolarized (13) C-acetoacetate. *Magn Reson Med.* **79,** 1862-1869
45. Sibille B, Keriel C, Fontaine E, Catelloni F, Rigoulet M, Leverve XM. (1995) Octanoate affects 2,4-dinitrophenol uncoupling in intact isolated rat hepatocytes. *Eur J Biochem.* **231,** 498-502
46. Berry MN, Phillips JW, Gregory RB, Grivell AR, Wallace PG. (1992) Operation and energy dependence of the reducing-equivalent shuttles during lactate metabolism by isolated hepatocytes. *Biochim Biophys Acta*. **1136**, 223-30
47. Davis EJ, Bremer J, Akerman KE. (1980) Thermodynamic aspects of translocation of reducing equivalents by mitochondria. *J Biol Chem.* **255,** 2277-83
48. LaNoue KF, Bryla J, Bassett DJ. (1974) Energy-driven aspartate efflux from heart and liver mitochondria. J Biol Chem. **249,** 7514-21
49. Qiu BY, Turner N, Li YY, Gu M, Huang MW, Wu F, Pang T, Nan FJ, Ye JM, Li JY, Li J. (2010) High-throughput assay for modulators of mitochondrial membrane potential identifies a novel compound with beneficial effects on db/db mice. *Diabetes.* **59,** 256-65
50. Hirst J. (2013) Mitochondrial complex I. *Annu Rev Biochem*. **82,** 551-75
51. Maldonado EN, DeHart DN, Patnaik J, Klatt SC, Gooz MB, Lemasters JJ. (2016) ATP/ADP turnover and import of glycolytic ATP into mitochondria in cancer cells is independent of the adenine nucleotide translocator. *J Biol Chem.* **291,** 19642-50
52. Zorova LD, Popkov VA, Plotnikov EY, Silachev DN, Pevzner IB, Jankauskas SS, Babenko VA, Zorov SD, Balakireva AV, Juhaszova M, Sollott SJ, Zorov DB. (2018) Mitochondrial membrane potential. *Anal Biochem.* **552,** 50-59
53. Pelantová H, Bugáňová M, Holubová M, Šedivá B, Zemenová J, Sýkora D, Kaválková P, Haluzík M, Železná B, Maletínská L, Kuneš J, Kuzma M. (2016) Urinary metabolomics profiling in mice with diet-induced obesity and type 2 diabetes mellitus after treatment with metformin, vildagliptin and their combination. Mol Cell Endocrinol. **431,** 88-100
54. Claus TH, Schlumpf JR, El-Maghrabi MR, Pilkis SJ. (1982) Regulation of the phosphorylation and activity of 6-phosphofructo 1-kinase in isolated hepatocytes by alpha-glycerolphosphate and fructose 2,6-bisphosphate. *J Biol Chem.* **257,** 7541-8
55. Agius L, Chowdhury MH, Davis SN, Alberti KG. (1986) Regulation of ketogenesis, gluconeogenesis, and glycogen synthesis by insulin and proinsulin in rat hepatocyte monolayer cultures. *Diabetes.* **35,** 1286-93
56. Stappenbeck R, Hodson AW, Skillen AW, Agius L, Alberti KG. (1990) Optimized methods to measure acetoacetate, 3-hydroxybutyrate, glycerol, alanine, pyruvate, lactate and glucose in human blood using a centrifugal analyser with a fluorimetric attachment. *J Automat Chem*. **12,** 213-20
57. Arden C, Petrie JL, Tudhope SJ, Al-Oanzi Z, Claydon AJ, Beynon RJ, Towle HC, Agius L. (2011) Elevated glucose represses liver glucokinase and induces its regulatory protein to safeguard hepatic phosphate homeostasis. *Diabetes.* **60,** 3110-20

FOOTNOTES AA was funded by HCED Iraq. LA acknowledges support from Diabetes UK (13/0004701)

Abbreviations: AOA, aminooxyacetate; DCIP, 2,6-dichlorophenol-indophenol; DHA, dihydroxyacetone; FBP1, fructose 1,6-bisphosphatase; FBPi, inhibitor of FBP1, 5-chloro-2-[N-(2,5dichlorobenzenesulfonamide)]-benzoxazole; G3P, glycerol 3-phosphate; GPi, inhibitor of mGPDH (ID STK017597); GP-shuttle, glycerophosphate shuttle; MA-shuttle, malate aspartate shuttle; mGPDH, mitochondrial FAD-dependent glycerol-3-phosphate dehydrogenase; PFK1, 6-phosphofructo-1-kinase; PFK2/FBP2, 6-Phosphofructose-2-kinase/fructose 2,6-bisphosphatase

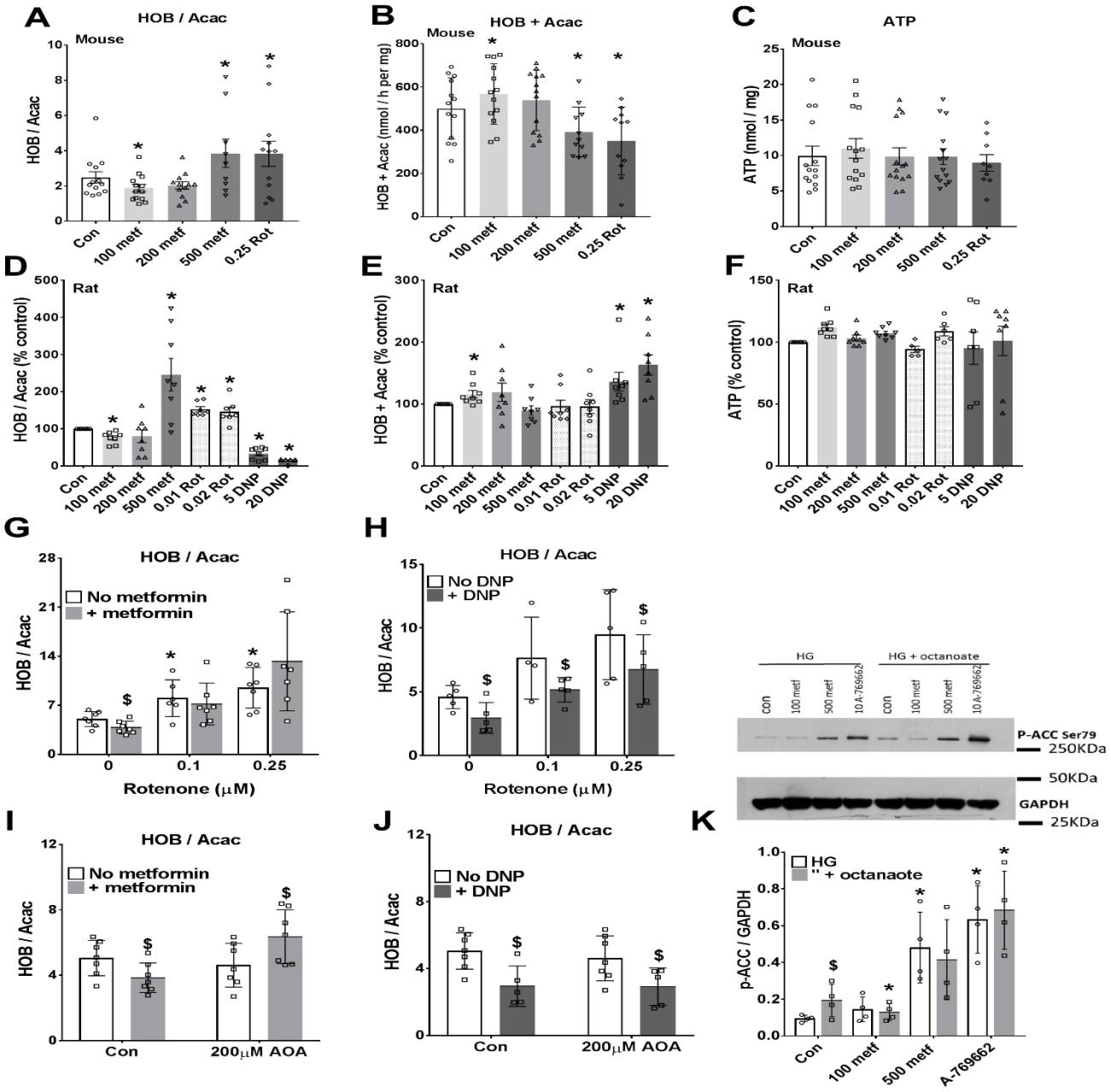

FIGURE 1. **Biphasic effect of metformin on the mitochondrial redox state: more oxidized at low metformin.** Mouse hepatocytes (A-C) and rat hepatocytes (D-F) were pre-cultured for 24h and then incubated for 2h in MEM with the metformin concentrations (100-500μM) indicated. The medium was then replaced with fresh MEM containing 25mM glucose, 0.25mM octanoate and the additions shown and incubations were for 1h. The medium was collected for analysis of acetoacetate (Acac) and D-3-hydroxybutyrate (HOB) and the cells were snap-frozen for ATP analysis. A,D ratio of 3-hydroxybutyrate / acetoacetate; B,E total production of acetoacetate + 3-hydroxybutyrate; C,F Cell ATP. Mouse data is expressed per mg protein and rat data as % control. Means ± SD for n= 8-14 hepatocyte preparations, *P < 0.05 relative to control.

G-J. Mouse hepatocytes cultured for 3h after cell plating then incubated for 2h without (open) or with (shaded) 100 μM metformin (G,I) and then for 1h in fresh MEM containing 25mM glucose + 0.125mM octanoate and the additions indicated: G and H effects of metformin (100 μM) or DNP, dinitrophenol (20μM) -/+ rotenone (0.1 or 0.25μM); I and J -/+ aminooxyacetate (200μM AOA). Means ± SD for n=5-7, * P < 0.05 relative to respective control; $, metformin or DNP effect. **K.** Immunoblot for phospho-ACC for mouse hepatocytes incubated -/+ metformin (100 or 500μM) and A-769662 (10μM) for 3h in MEM with 25mM glucose (HG) -/+ 0.125mM octanoate for the last h. Representative Immunoblot and densitometry for n=4 mouse hepatocyte preparations, * P < 0.05 relative to respective control; $ P < 0.05 octanoate effect.

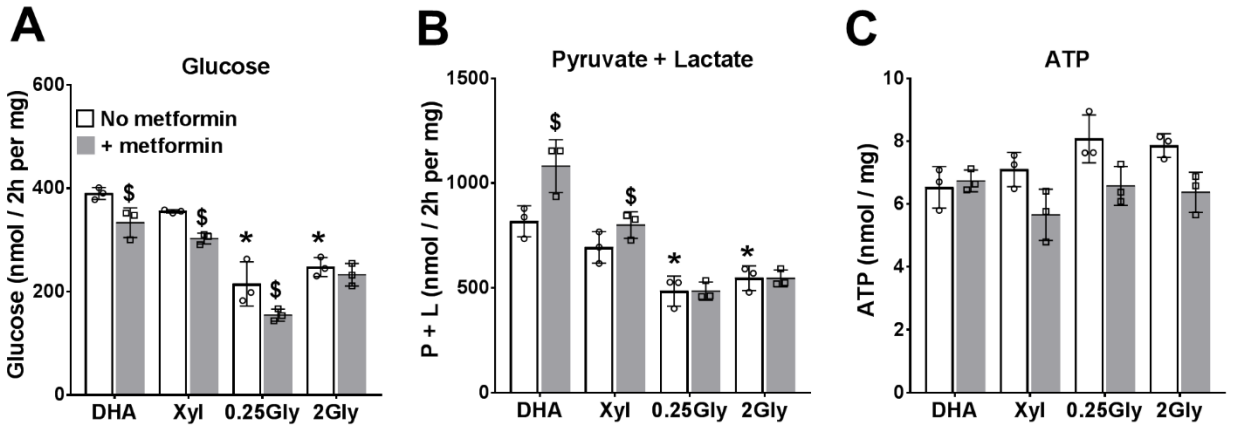

FIGURE 2. **Effects of metformin on glucose production from oxidized and reduced substrates.** After overnight culture, mouse hepatocytes were pre-incubated for 2h in glucose-free DMEM without or with 100µM metformin. The medium was then replaced by fresh glucose-free DMEM containing either 5mM DHA, 2mM xylitol (Xyl) or glycerol at 0.25mM or 2mM. After 2h the medium was collected for determination of glucose (A), pyruvate and lactate (B) and cell ATP (C). Means ± SD for triplicate plates from 1 hepatocyte isolation. * *P < 0.05* relative to DHA; $, metformin effect.

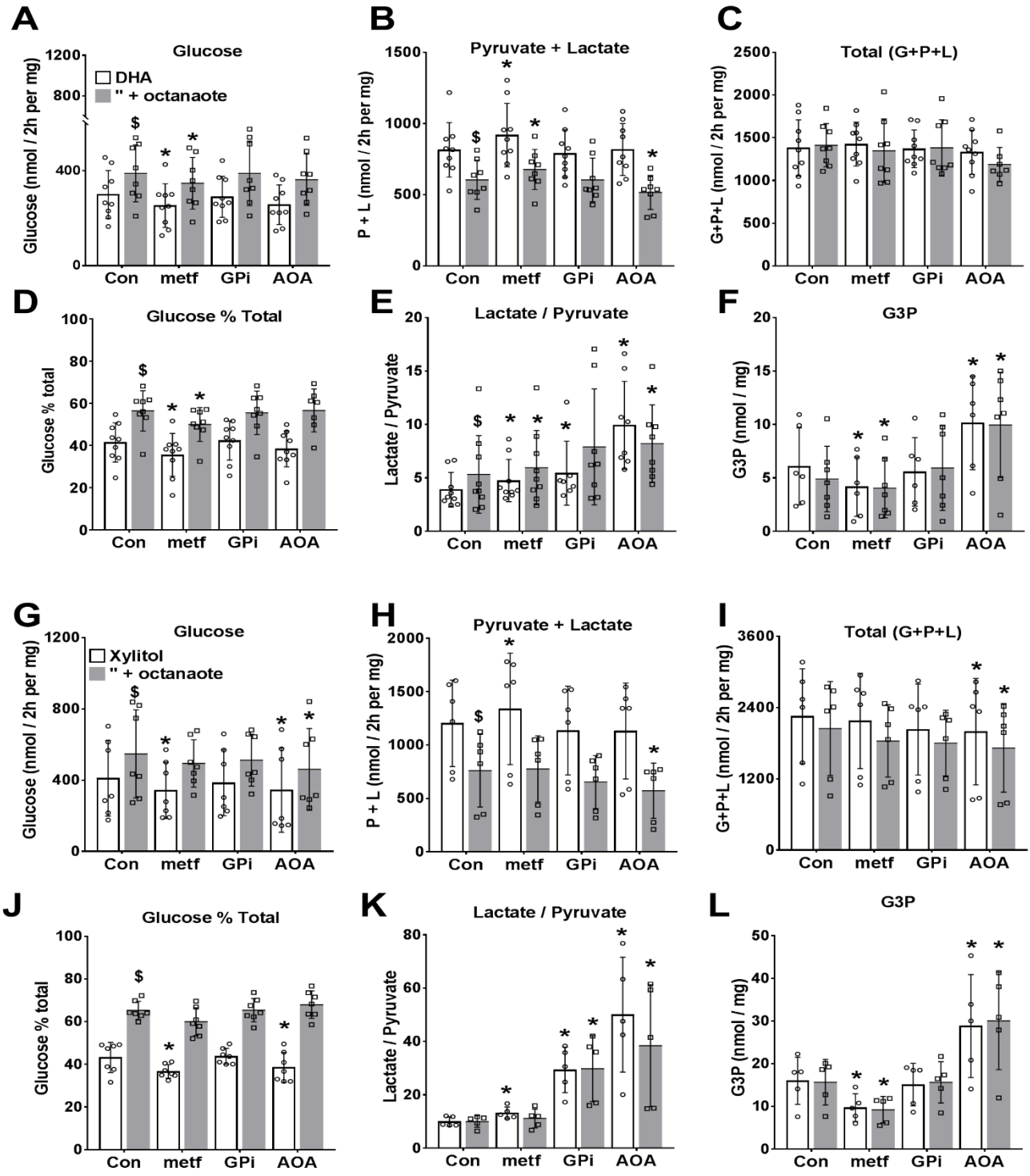

FIGURE 3. **Dihydroxyacetone and xylitol metabolism to glucose, pyruvate and lactate: effects of metformin and NADH shuttle inhibitors.** Mouse hepatocytes were pre-incubated for 2h in glucose-free DMEM. The medium was then replaced by fresh medium containing either 5mM DHA (**A-F**) or 2mM xylitol (**G-L**) either without (open bars) or with (shaded bars) 0.125mM octanoate and other additions as shown and incubation was for 2h. Metformin (100µM) and GPi (20µM) were present during both pre-incubation and final incubation and aminooxyacetate (AOA, 200µM) only in the final incubation. **A,G.** Glucose production; **B,H.** Pyruvate + lactate production; **C,I.** total production of glucose + pyruvate + lactate, expressed as C3 units; **D,J**. Glucose % total metabolism; **E,K.** lactate / pyruvate ratio; **F,L.** Cell G3P. Means ± SD for n= 6-9 (A-F) or 5-7 (G-L) hepatocyte preparations, * $P < 0.05$ relative to respective control; $ $P < 0.05$ octanoate effect.

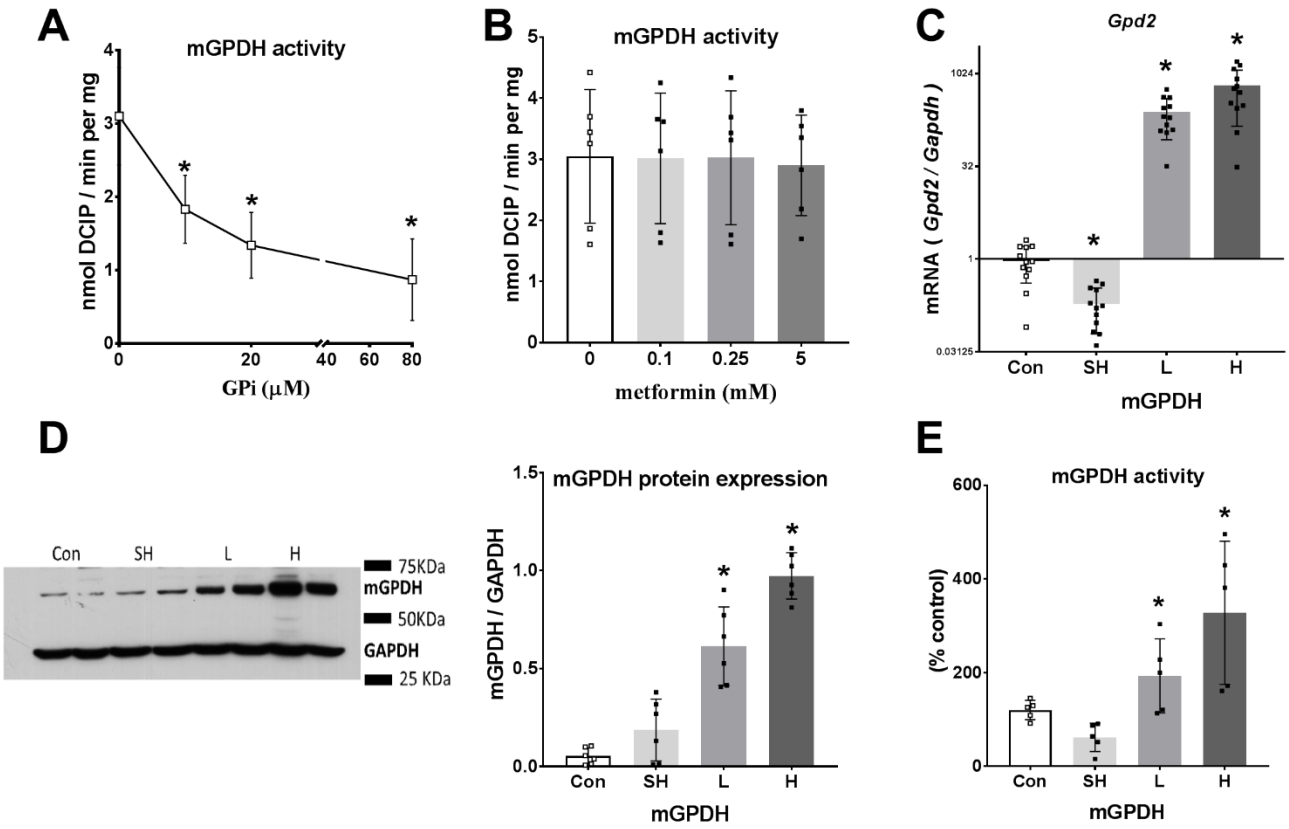

FIGURE 4. **Endogenous mGPDH activity and effects of GPi and metformin.** A.B. Activity of endogenous mGPDH assayed in permeabilised hepatocytes with the concentrations of GPi (**A**) or metformin (**B**) indicated**. C-E.** Hepatocytes were either untreated (Con) or treated with 8 x 10^8 PFU/ml Adv-SH-mGpd2 (SH) for *Gpd2* knock-down or with Adv-mGpd2 at 1.6 (L) or 4.8 (H) x 10^7 PFU/ml for mGPDH overexpression. **C.** *Gpd2/Gapdh* mRNA expressed relative to untreated control. **D.** Immunoactivity of mGPDH/GAPDH. **E** mGPDH enzyme activity. Means ± SD for n= 6-12 (A,B) or 5-6 (C-E) experiments, * $P < 0.05$ relative to control.

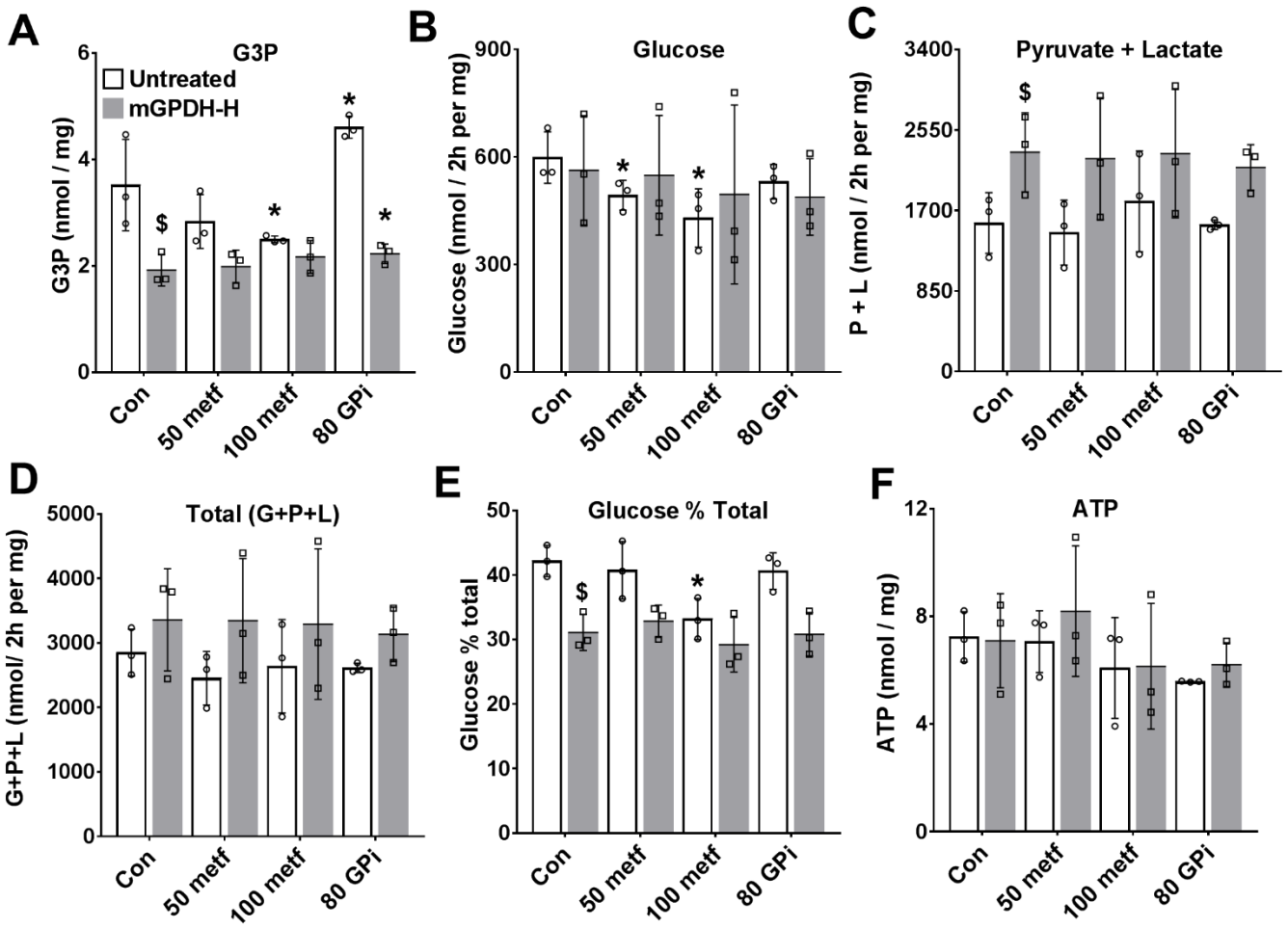

FIGURE 5. **The mGPDH inhibitor raises cell G3P but does not mimic metformin.** Mouse hepatocytes were either untreated or treated with Adv-m*Gpd2* at 4.8 x 10^7 PFU/ml (mGPDH-H) for overexpression of mGPDH as in Fig. 4. After overnight culture they were incubated for 2h in glucose-free DMEM with 50µM or 100µM metformin or with 80µM GPi (STK017597) as indicated. They were then incubated in fresh medium containing 5mM DHA and the same metformin and GPi concentrations for determination of glucose, pyruvate and lactate production. A. Cell G3P; B. Glucose production; **C.** Pyruvate + lactate production; **D.** Total production of glucose, pyruvate and lactate (C3 units); **E.** Glucose % total metabolism; **F.** Cell ATP. Means ± SD for 3 hepatocyte preparations. * $P < 0.05$ relative to respective control; $ < 0.05 effect of mGPDH overexpression.

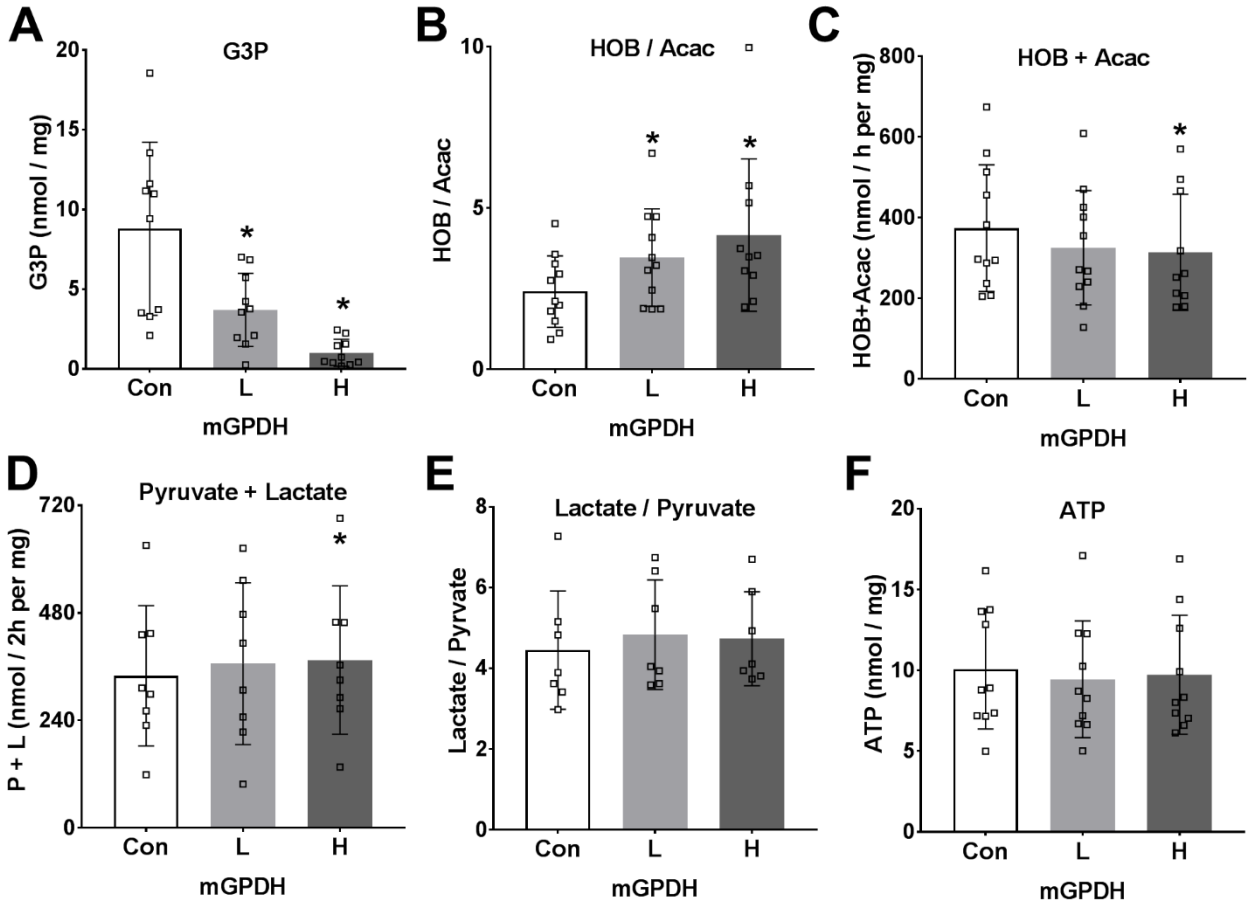

FIGURE 6. **Overexpression of mGPDH in hepatocytes promotes lower G3P, a reduced mitochondrial NADH / NAD redox state and increased glycolysis.** Mouse hepatocytes were either untreated (Con) or treated with low (L) and high (H) titres of Adv-Gpd2 for overexpression of mGPDH as in Fig. 4. After 20 h culture to allow protein overexpression they were incubated for 1 h in MEM containing 25mM glucose and 0.125mM octanoate. A. G3P; B, C. 3-hydroxybutyrate / acetoacetate ratio and total 3-hydroxybutyrate + acetoacetate production; D,E. Pyruvate and lactate production and lactate / pyruvate ratio; F. Cell ATP. Means ± SD for n= 7-11, * $P < 0.05$ relative to untreated control.

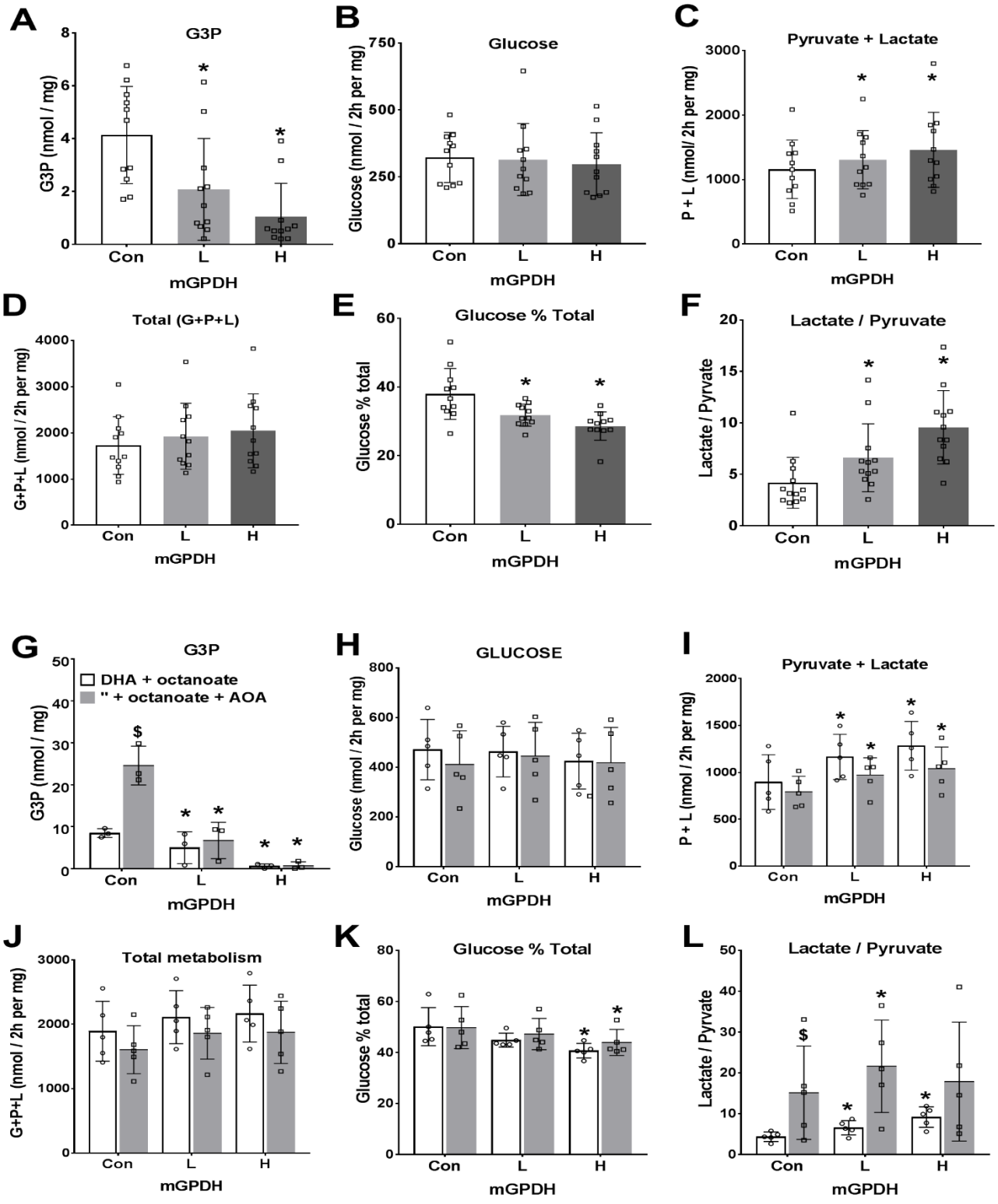

FIGURE 7. **Overexpression of mGPDH favours metabolism of dihydroxyacetone to pyruvate and lactate rather than glucose.** Mouse hepatocytes were either untreated or treated for overexpression of mGPDH (L and H) as in Fig. 4 and 5. After 20h culture they were incubated for 2h in glucose-free DMEM containing either 5mM DHA (A-F) or 5mM DHA and 0.125mM octanoate (G-L) without (open bar) or with(shaded bar) 200µM AOA. A,G. Cell G3P; B,H. Glucose production; C,I. Pyruvate + lactate; D,J, total production of glucose + pyruvate + lactate expressed as C3 units; E,K. Glucose % total metabolism; F,L. lactate / pyruvate ratio. Means ± SD for n= 11-12 (A-F) or n= 3-5 (G-L), * $P < 0.05$ effect of mGPDH overexpression, $ $P < 0.05$ effect of AOA.

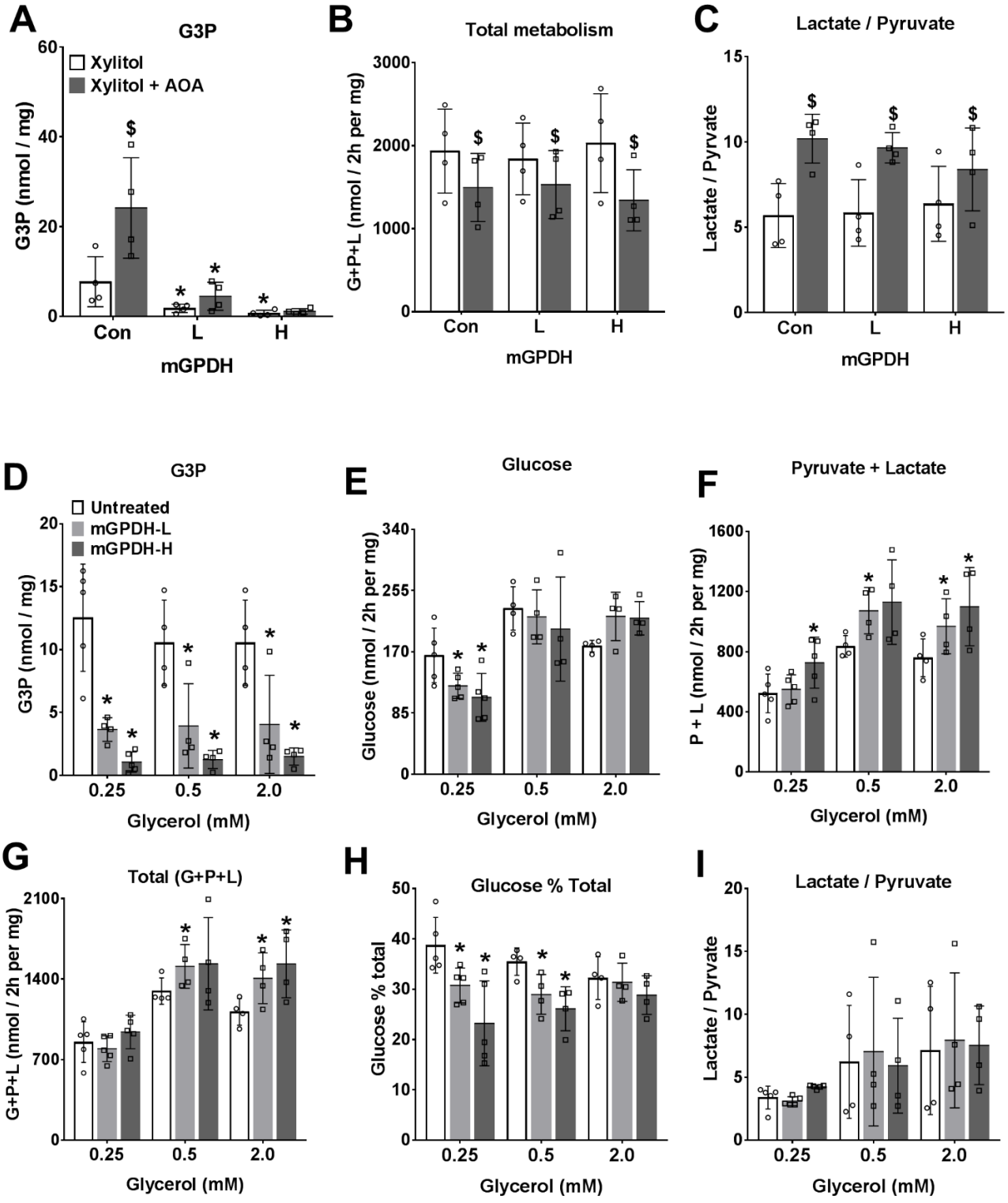

FIGURE 8. **Overexpression of mGPDH favours increased glycerol but not xylitol metabolism.** Mouse hepatocytes were either untreated or treated for overexpression of mGPDH (L and H) as in Fig. 4 and cultured for 20h followed by 2h incubation in glucose-free DMEM. A-C. Medium contained 2mM xylitol without (open bar) or with (shaded bar) 200µM aminooxyacetate (AOA). A, Cell G3P; B. total production of glucose + pyruvate + lactate expressed as C3 units; C. lactate / pyruvate ratio. D-I. Medium contained glycerol at either 0.25, 0.5 or 2mM. D, Cell G3P; E. Glucose production; F. Pyruvate + lactate; G, total production of glucose + pyruvate + lactate (C3 units); H. Glucose % total metabolism; I. lactate / pyruvate ratio. Means ± SD for n= 4-5, * *P < 0.05* effect of mGPDH overexpression (A-I); $ *P < 0.05* effect of AOA (A-C)

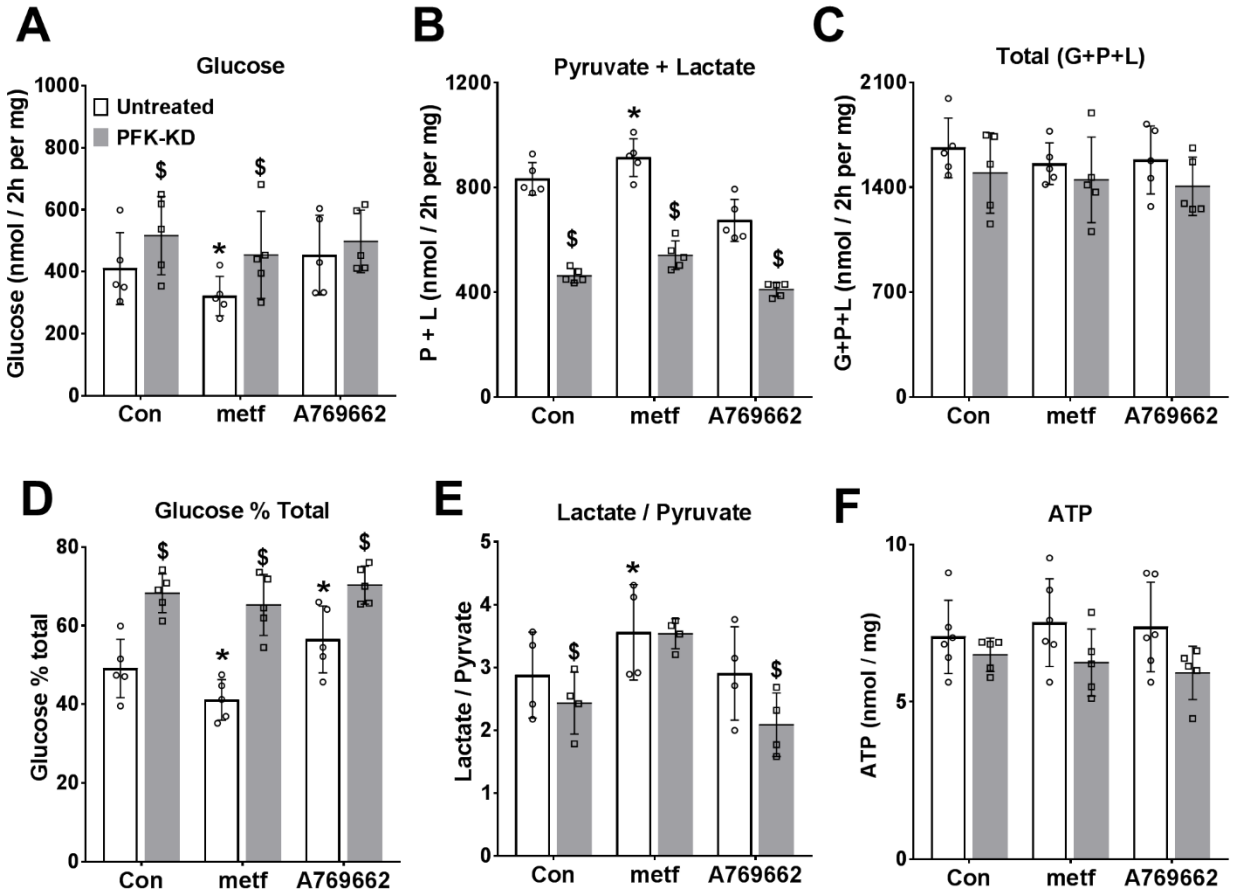

FIGURE 9. **Comparison of metformin and an AMPK activator on DHA metabolism in cells depleted of fructose 2,6-P_2.** Mouse hepatocytes were either untreated (open bars) or treated (filled bars) with an adenoviral vector for expression of kinase-deficient PFK2 (PFK-KD) to deplete cell fructose 2,6-P_2 (38). After 20 h culture they were pre-incubated for 2h in glucose-free medium with 100µM metformin or 10µM A-769662. They were then incubated for 2h in fresh medium containing 5mM DHA. **A.** Glucose production; **B.** Pyruvate + lactate production; **C.** total production of glucose + pyruvate + lactate (C3 units); **D**. Glucose % total metabolism; **E.** lactate / pyruvate ratio; **F.** Cell ATP. Means ± SD for n= 4-6, * $P < 0.05$; relative to respective control; $, effect of PFK-KD.

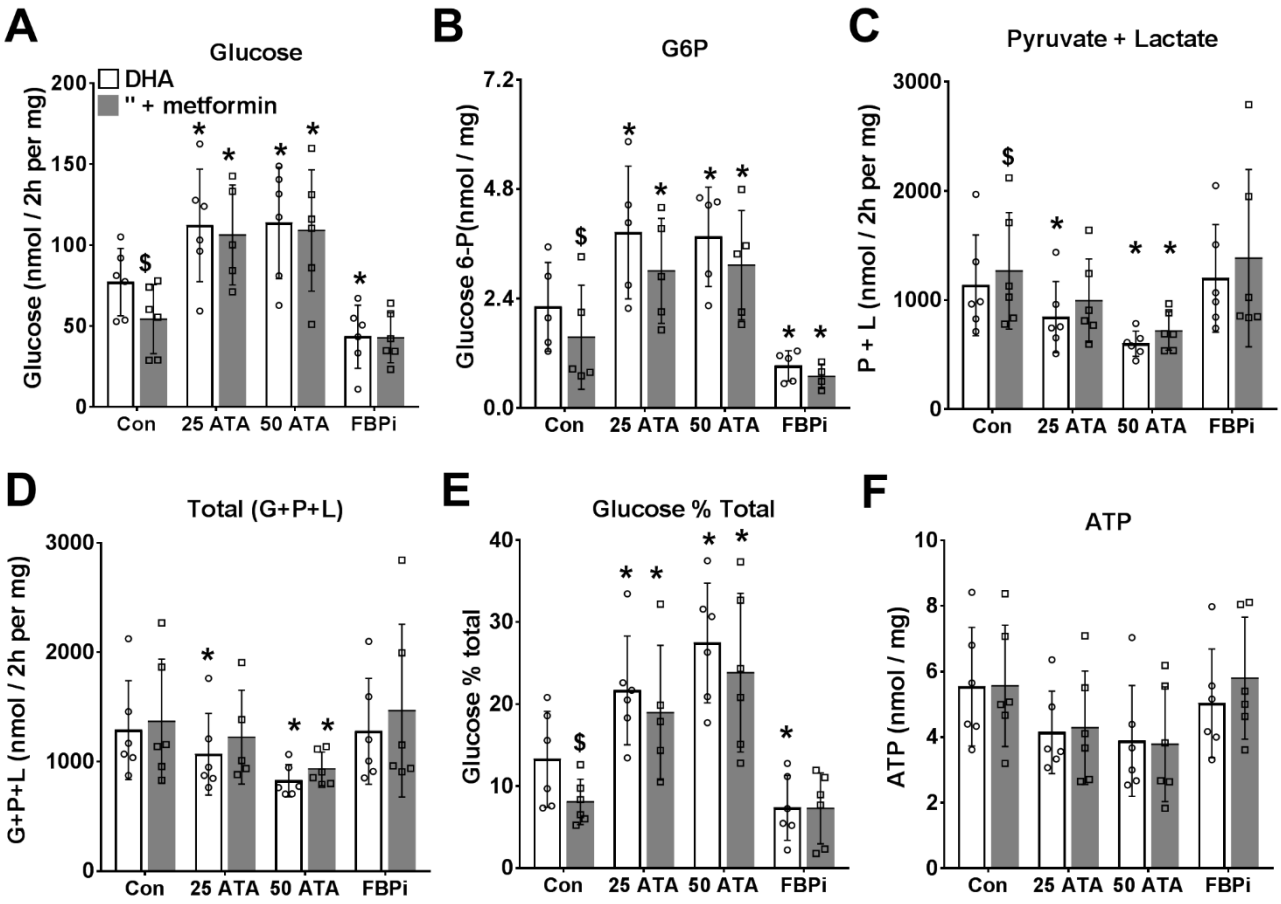

FIGURE 10. **Metformin inhibition of gluconeogenesis from DHA is abolished by inhibitors of PFK1 or FBP1.** Mouse hepatocytes were incubated for 2h in glucose-free DMEM without (open) or with (shaded) 100µM metformin and then for 2h in fresh medium containing 5mM DHA + 200nM S4048 and other additions as indicated: aurintricarboxylic acid (ATA) at 25 or 50µM and FBPi at 5µM. A. Glucose production; B Cell glucose 6-P; C. Pyruvate + lactate production; D; total production of glucose + pyruvate + lactate, as C3 units; E. Glucose % total metabolism; F. Cell ATP. Means ± SD for n= 5-6, * $P < 0.05$ relative to respective control; $ $P < 0.05$ metformin effect.

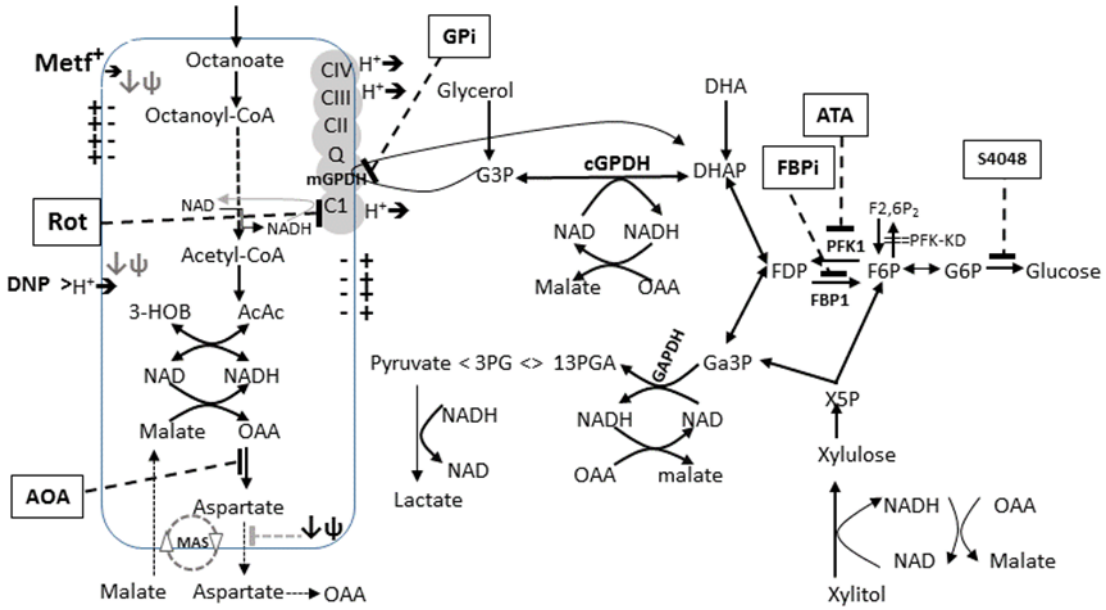

FIGURE 11. **Substrate and inhibitor effects on the NADH/NAD redox state.** *Octanoate* is metabolised in mitochondria by β-oxidation generating NADH and FADH, which are oxidised in the electron transport chain, and the final end-products: acetoacetate (Acac) and 3-hydroxybutyrate (HOB). The ratio of HOB/Acac reflects the mitochondrial NADH/NAD redox state. It is increased by high metformin and rotenone (Complex I inhibitor) and decreased by low metformin and uncoupler, DNP (***Fig. 1***). It is increased by overexpression of mGPDH which catalyses oxidation of G3P with transfer of electrons to the respiratory chain (***Fig. 6***). *DHA* is metabolised to either glucose or pyruvate. The latter results in production of NADH (at GAPDH) which is coupled to either formation of lactate by lactate dehydrogenase or malate, which is oxidised in mitochondria by the malate-aspartate-shuttle (MAS) (***Fig. 3,7***). *Xylitol* metabolism generates NADH during oxidation to xylulose and at GAPDH during formation of pyruvate (***Fig. 3,8***). *Glycerol* metabolism generates G3P which is converted to DHAP by either mGPDH, with transfer of electrons to the respiratory chain or by cGPDH generating NADH in the cytoplasm which re-oxidized via the MA-shuttle (***Fig. 8***). *AOA* inhibits the MA-shuttle at the transaminase reaction and increases the lactate / pyruvate ratio and G3P and inhibits total xylitol metabolism (***Fig. 3,7,8***). The MA-shuttle is also inhibited at the aspartate transport step by mitochondrial depolarisation (↓ψ). GPi (80 µM, mGPDH inhibitor) increases G3P (***Fig. 5***). *mGPDH* overexpression lowers G3P, increases total glycerol metabolism and favours DHA metabolism to pyruvate and lactate relative to glucose (***Fig. 6-8***). *Octanoate, ATA* (PFK1 inhibitor) and fructose 2,6-P_2 depletion promote DHA metabolism to glucose relative to pyruvate and lactate (***Fig. 9,10***). *Metformin* (100 µM or < 2nmol/mg cell protein) promotes decreased DHA metabolism to glucose relative to pyruvate plus lactate and moderately increases the lactate / pyruvate ratio and decreases cell G3P (***Figs 3,5,9,10***). It lowers G6P in conditions of restrained G6P entry into the endoplasmic reticulum with a transport inhibitor, S4048 (***Fig. 10***).

Low metformin causes a more oxidized mitochondrial NADH/NAD redox state in hepatocytes and inhibits gluconeogenesis by a redox-independent mechanism

Ahmed Alshawi and Loranne Agius

J. Biol. Chem. published online December 27, 2018
